AIP Advances

Mixed conductivity analysis of single crystals of α'''-$(Cd_{1-x}\ Zn_x)_3As_2$ (x = 0.45)

Cite as: AIP Advances **11**, 035028 (2021); https://doi.org/10.1063/5.0038477
Submitted: 26 November 2020 . Accepted: 25 February 2021 . Published Online: 11 March 2021

V. S. Zakhvalinskii, T. B. Nikulicheva, A. V. Kochura, E. Lahderanta, M. Shakhov, A. S. Kubankin, M. Sukhov, M. N. Yaprintsev, and A. A. Morocho

Mixed conductivity analysis of single crystals of α'''-$(Cd_{1-x}Zn_x)_3As_2$ (x = 0.45)

Cite as: AIP Advances 11, 035028 (2021); doi: 10.1063/5.0038477
Submitted: 26 November 2020 • Accepted: 25 February 2021 •
Published Online: 11 March 2021

V. S. Zakhvalinskii,[1,a] T. B. Nikulicheva,[1,b] A. V. Kochura,[2] E. Lahderanta,[3] M. Shakhov,[4] A. S. Kubankin,[1] M. Sukhov,[1] M. N. Yaprintsev,[1] and A. A. Morocho[1]

AFFILIATIONS

[1] Belgorod National Research University, Belgorod 308015, Russia
[2] SouthWest State University, Kursk 305040, Russia
[3] Department of Mathematics and Physics, Lappeenranta University of Technology, P.O. Box 20, FIN-53852 Lappeenranta, Finland
[4] Ioffe Institute, 26 Politekhnicheskaya, St. Petersburg 194021, Russia

[a] zakhvalinskii@bsu.edu.ru
[b] Author to whom correspondence should be addressed: nikulicheva@bsu.edu.ru

ABSTRACT

We study the conductivity and magnetoresistance of the α''' phase solid solution of $(Cd_{1-x}Zn_x)_3As_2$ (x = 0.45). Single crystals of $(Cd_{1-x}Zn_x)_3As_2$ are obtained by the modified Bridgman method. The space group and tetragonal lattice parameters of single crystals are found to be $I4_1/amd$ and $a = b = 8.56(5)$ Å, $c = 24.16(6)$ Å. The temperature dependence of the conductivity and magnetoresistance is studied in the temperature range of 1.6–320 K and in the presence of a transverse magnetic field from 0 to 10 T. Mixed conductivity is analyzed using Hall resistivity data and standard quantitative mobility spectrum analysis. The concentration and mobility of holes are determined at different temperatures. The presence of two types of holes with different mobilities is demonstrated in the temperature range of 1.6–19 K, while with increasing temperature, just one type of charge carrier is observed in the mobility spectrum.

I. INTRODUCTION

Cadmium and zinc pnictides (including both the semimetal Cd_3As_2 and the semiconductor Zn_3As_2) belong to the class of II–V semiconductor compounds and have a well-defined set of interesting characteristics, including structural, optical, and transport properties.[1] These compounds have long been known as materials with a variety of practical applications,[2–5] and their properties are the subject of considerable current research activity. Although Cd_3As_2 and Zn_3As_2 have similar crystal structures, the ordering of deformed antifluorite cubes differs between them. After the discovery of the topological properties of Cd_3As_2,[6,7] considerable research effort was focused on the topological properties of solid solutions of $(Cd_{1-x}Zn_x)_3As_2$[8] and solid solutions of dilute magnetic semiconductors based on Cd_3As_2.[9,10] On the other hand, composite materials based on Cd_3As_2 have been investigated owing to their applications in spintronics.[11] It is well known that $(Cd_{1-x}Zn_x)_3As_2$ solid solutions in the composition range $0 \le x \le 0.6$ undergo structural transformations (from the space group $I4_1/acd$ to $P4_2/nmc$ and then back to $I4_1/acd$) with increasing Zn content.[8] All the studied samples of $(Cd_{1-x}Zn_x)_3As_2$ belong to the tetragonal system (α''-Cd_3As_2) and space group $P4_2/nmc$ (ICSD Database, Version 2009-1, Ref. Code 23 245).[9,10]

In the quasi-binary system Cd_3As_2–Zn_3As_2, there is a continuous series of solid solutions,[12] and the state diagram of Cd_3As_2–Zn_3As_2 shows a region of existence of α''' solid solution phases of $(Cd_{1-x}Zn_x)_3As_2$ in the composition range $0.45 \le x \le 0.65$;[6] this region is a poorly studied area in condensed-matter systems. In Ref. 13, single crystals of α'''-$(Zn_{1-x}Cd_x)_3As_2$ (x = 0.26) were obtained and studied by x-ray diffraction analysis, and the following tetragonal lattice parameters were found: $a = b = 8.5377(2)$ Å, $c = 24.0666(9)$ Å, space group $I4_1/amd$, and $Z = 16$.

Although properties such as the electrical conductivity and magnetoresistance of the α''' phases of $(Cd_{1-x}Zn_x)_3As_2$ have not been studied in great detail, it is well known that an increase in the Zn content of solid solutions leads to a transition from the Dirac

semiconductor Cd_3As_2 to the direct-gap semiconductor Zn_3As_2. In this case, not only does the type of the majority charge carriers change from *n* to *p* but also the nature of the temperature dependence of the electrical conductivity changes. It has been shown in magnetoresistance studies of solid solutions that with increasing Zn content, a transition from topological to ordinary semiconductor properties occurs.[8] Thus, the presence of Shubnikov–de Haas (SdH) oscillations both in the narrow-gap semiconductor Cd_3As_2 with an inverted band structure and in $(Cd_{1-x}Zn_x)_3As_2$ solid solutions makes it possible to analyze the evolution of the topological properties as the composition changes.[8] Based on the Bodnar model for the semiconductors Cd_3As_2 and Zn_3As_2,[14] it is also possible to track the evolution of the band structure from 0.1 to 1.0 eV,[15,16] as well as the changes in the contributions of different groups of charge carriers to the magnetoresistance.

In single crystals of α'''-$(Cd_{1-x}Zn_x)_3As_2$ (X = 0.45), the magnetic field dependence of the resistivity at different temperatures does not exhibit SdH oscillations, in contrast to compositions with $x \leq 0.38$.[8] For this reason, we have analyzed the mixed conductivity using experimental data on changes in Hall resistivity in the presence of a magnetic field. In this work, we use standard quantitative mobility spectrum analysis (QMSA).[17–20]

II. EXPERIMENTAL

$(Cd_{1-x}Zn_x)_3As_2$ single crystals with X = 0.45 were grown by the modified Bridgeman method from stoichiometric amounts of Cd_3As_2 and Zn_3As_2. The crystals under study were slow-cooled at a rate of 5 °C/h and in the presence of a temperature gradient near the melting point (T = 853 °C). High degree stoichiometry of the compounds Cd_3As_2 and Zn_3As_2 is achieved by additional sublimation in the vapor phase. The composition and homogeneity of the samples were monitored by X-ray powder diffraction (XRD) analysis using a SmartLab diffractometer (Rigaku, Japan) with an angular range from 60° to 80°, step = 0.001, v = 0.5°/min, and a Cu anode (λ = 0.154 059 290 nm). The $(Cd_{1-x}Zn_x)_3As_2$ single crystals exhibited high crystallinity with tetragonal lattice parameters $a = b$ = 8.56(5) Å, c = 24.16(6) Å, space group $I4_1/amd$, and Z = 16.

The XRD pattern of the $(Cd_{1-x}Zn_x)_3As_2$ (x = 0.45) powder measured in θ–2θ mode is shown in Fig. 1. According to the phase diagram of solid solutions of Cd_3As_2–Zn_3As_2 in the composition range $x \approx 0.4$–0.8 at room temperature,[21] a solid solution of $(Cd_{1-x}Zn_x)_3As_2$ can crystallize into the α''' phase with a tetragonal structure (space group $I4_1/amd$), which is related to a fluorite structure.[13] From the coordinates of the basis atoms, obtained in Ref. 13 for a composition with a predominance of zinc arsenide [$(Zn_{1-x}Cd_x)_3As_2$, x = 0.26], and using the PowderCell program,[22] it was possible to index the main crystallographic planes from which the diffraction occurred.

The matched planes show very good agreement with the peak positions shown in Fig. 1. Thus, a determination of the lattice parameters of the investigated sample $(Cd_{1-x}Zn_x)_3As_2$ (X = 0.45) was carried out for the α''' crystal structure, and these were found to be $a = b$ = 8.56(5) Å and c = 24.16(6) Å. These parameters are larger than the values [a = 8.5377(2) Å and c = 24.0666(9) Å] determined in Ref. 13 from x-ray diffraction studies of a solid solution with a lower content of cadmium arsenide, $(Zn_{1-x}Cd_x)_3As_2$ (x = 0.26). Zn and Cd ions are randomly distributed in the α''' structure over three

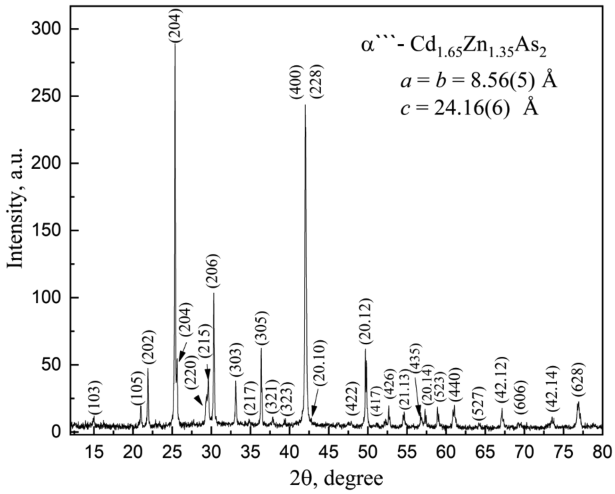

FIG. 1. XRD pattern of $(Cd_{1-x}Zn_x)_3As_2$ (X = 0.45).

independent positions with tetrahedral coordination (fourfold coordination), for which the ionic radii are 0.6 and 0.78 Å, respectively.[23] Therefore, an increase in the degree of substitution of Cd ions for Zn ions leads to an increase in the lattice parameters, a phenomenon that was observed earlier for other polymorphic modifications of Cd_3As_2–Zn_3As_2 solid solutions.[21,24]

The $(Cd_{1-x}Zn_x)_3As_2$ samples were 1 × 1 × 5 mm^3 right-rectangular prisms with soldered thin electrodes. Measurements of the temperature dependence of the magnetoresistance were made in the presence of a transverse magnetic field configuration 0–10 T and over the temperature range of 1.6–320 K using the six-probe method. For measurements, the sample probe was inserted into a He-exchange-gas Dewar, where the temperature could be adjusted with an accuracy of 0.5%.

Figure 2 shows the magnetic field dependence of resistivity at different temperatures for $(Cd_{1-x}Zn_x)_3As_2$ (x = 0.45).

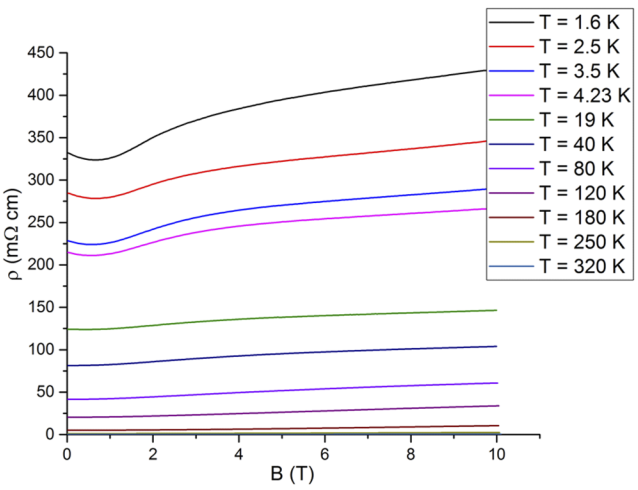

FIG. 2. Magnetic field dependence of the resistivity of $(Cd_{1-x}Zn_x)_3As_2$ (x = 0.45).

III. RESULTS AND DISCUSSION

For single-carrier materials, the Hall coefficient and resistivity are defined as

$$R_H(B) = \frac{1}{nq}, \tag{1}$$

$$\rho(B) = \frac{1}{nq\mu}, \tag{2}$$

respectively, where n is the carrier concentration, μ is the mobility, q is the carrier charge, and B is the magnetic field. When there is just one type of carrier, the conductivity tensor is calculated as

$$\sigma_{xx} = \frac{nq\mu}{1+\mu^2B^2}, \tag{3}$$

$$\sigma_{xy} = \frac{nq\mu^2B}{1+\mu^2B^2}. \tag{4}$$

When different types of carriers are present, the carrier mobility and density calculated from Eqs. (1) and (2) are the values averaged over all carriers. For such materials, the specific electrical conductivities of individual carriers are additive, and the total conductivity tensor (for systems with N carriers) is defined as

$$\sigma_{xx}^{\exp} = \sum_{j=1}^{N} \frac{n_j q_j \mu_j}{1+\mu_j^2B^2}, \tag{5}$$

$$\sigma_{xy}^{\exp} = \sum_{j=1}^{N} \frac{n_j q_j \mu_j^2 B}{1+\mu_j^2B^2}. \tag{6}$$

The validity of Eqs. (5) and (6) depends on two assumptions, which do not always hold. First, it is assumed that the carrier concentration and mobility are independent of the magnetic field, but, strictly speaking, this is not always true. For example, a magnetic-field-dependent shift of the energy gap can lead to a significant change in concentration of intrinsic carriers[25] or the effective mobility can decrease strongly with increasing magnetic field owing to the phenomenon of magnetic freezing.[26] Second, Eqs. (5) and (6) have been obtained from a semiclassical approach, but the discreteness of the Landau levels means that SdH oscillations (and sometimes the quantum Hall effect) are superimposed on classical conductivity. Thus, SdH oscillations often dominate in transport processes at high fields and/or low temperatures and are insignificant at low fields or high temperatures owing to an increased number of collisions and to thermal expansion, respectively. Consequently, the data obtained from the quantum Hall effect are not suitable for rigorous analysis of mixed conductivity when it is not possible to remove SdH oscillations. However, at the same time, SdH oscillations and the quantum Hall effect themselves provide valuable information complementary to that obtained from semiclassical analysis of mixed conductivity.

Mobility spectrum analysis (MSA) considers the conductive spectrum as a function of mobility from the relationship between the conductivity tensor and the magnetic field strength. In this spectrum, each peak value corresponds to the contribution from one of the carriers, and the sign of the mobility indicates the carrier type.[27] When applying MSA, it is first assumed that the mobilities of electrons and holes in the samples are continuously distributed. Equations (5) and (6) can then be replaced by integrals,

$$\sigma_{xx}(B) = \int_0^\infty \frac{s^p(\mu) + s^n(\mu)}{1+\mu^2B^2} d\mu, \tag{7}$$

$$\sigma_{xy}(B) = \int_0^\infty \frac{[s^p(\mu) - s^n(\mu)]\mu B}{1+\mu^2B^2} d\mu. \tag{8}$$

Dziuba and Górska[28] proposed that Eqs. (7) and (8) should be solved by an iterative approximation method. In accordance with this, the integrals in these equations are replaced by Riemann sums,

$$\sigma_{xx}(B) = \sum_{i=1}^{m} \frac{[s^p(\mu_i) + s^n(\mu_i)]\Delta\mu_i}{1+\mu_i^2B^2} = \sum_{i=1}^{m} \frac{S_i^{xx}\Delta\mu_i}{1+\mu_i^2B^2}, \tag{9}$$

$$\sigma_{xy}(B) = \sum_{i=1}^{m} \frac{[s^p(\mu_i) - s^n(\mu_i)]\mu_i B\Delta\mu_i}{1+\mu_i^2B^2} = \sum_{i=1}^{m} \frac{S_i^{xy}\mu_i B\Delta\mu_i}{1+\mu_i^2B^2}, \tag{10}$$

where m is the number of discrete mobilities into which the mobility spectrum is subdivided. The functions S_i^{xx} and S_i^{xy} are defined as

$$S_i^{xx} = s^p(\mu_i) + s^n(\mu_i), \tag{11}$$

$$S_i^{xy} = s^p(\mu_i) - s^n(\mu_i). \tag{12}$$

The Jacobi iterative method is used to solve Eqs. (9) and (10) and obtain the mobility spectrum. In this method, the range of mobility depends on the magnetic field used for the measurement. The upper and lower bounds satisfy the conditions $1/B_{\max}^{\exp} \le \mu \le 1/B_{\min}^{\exp}$. In accordance with the Jacobi iterative procedure, Eqs. (9)–(12) are transformed to the form

$$S_i^{xx} = \left(1+\mu_i^2B^2\right)\left[\sigma_{xx}^{\exp}(B_i) - \sum_{j=1}^{i-1} \frac{S_j^{xx}}{1+\mu_j^2B_i^2} - \sum_{j=i+1}^{m} \frac{S_j^{xx}}{1+\mu_j^2B_i^2}\right], \tag{13}$$

$$S_i^{xy} = \frac{\left(1+\mu_i^2B^2\right)}{\mu_i B_i}\left[\sigma_{xy}^{\exp}(B_i) - \sum_{j=1}^{i-1} \frac{S_j^{xy}\mu_j B_i}{1+\mu_j^2B_i^2} - \sum_{j=i+1}^{m} \frac{S_j^{xx}\mu_j B_i}{1+\mu_j^2B_i^2}\right]. \tag{14}$$

At each point of the subregion, the carrier parameters are determined by the linear least squares method,

$$\chi^2 = \sum_{i}^{m}\left[\left(\sigma_{xx}^{\exp}(B_i) - \sum_{j}^{N}\sigma_{xx}^{j}(B_i)\right)^2 + \left(\sigma_{xy}^{\exp}(B_i) - \sum_{j}^{N}\sigma_{xy}^{j}(B_i)\right)^2\right]. \tag{15}$$

The subregion point with the minimum value is used as the initial approximation, and the Goldstein–Armijo rule is used to select the

step. Then, to accelerate convergence, the relaxation method is used to solve the linear equations (13) and (14),

$$S_i^{xx}(k+1) = (1-\omega_{xx})S_i^{xx}(k) + \omega_{xx}\left(1+\mu_i^2B^2\right) \times \left[\sigma_{xx}^{\exp}(B_i) - \sum_{j=1}^{i-1}\frac{S_j^{xx}(k+1)}{1+\mu_j^2B_i^2} - \sum_{j=i+1}^{m}\frac{S_j^{xx}(k)}{1+\mu_j^2B_i^2}\right], \quad (16)$$

$$S_i^{xy}(k+1) = (1-\omega_{xy})S_i^{xx}(k) + \omega_{xy}\frac{\left(1+\mu_i^2B^2\right)}{\mu_iB_i} \times \left[\sigma_{xy}^{\exp}(B_i) - \sum_{j=1}^{i-1}\frac{S_j^{xy}(k+1)\mu_jB_i}{1+\mu_j^2B_i^2} - \sum_{j=i+1}^{m}\frac{S_j^{xy}(k)\mu_jB_i}{1+\mu_j^2B_i^2}\right], \quad (17)$$

where $S_i^{xx}(k)$ and $S_i^{xy}(k)$ are the results from the kth iteration step, and both ω_{xx} and ω_{xy} give the convergence rate of the iterative procedure (the relaxation rate). To determine the optimal value of ω_{xx}, the following estimation procedure is used.[29]

If $\Delta S_i^{xx} = S_i^{xx}(k+1) - S_i^{xx}(k)$ is the change during the kth iteration performed without relaxation (i.e., with $\omega_{xx} = 1$), then

$$(\omega_{xx})_{\text{opt}} \approx \frac{2}{1+\sqrt{1-\left(\Delta S_i^{xx}(k+p)/\Delta S_i^{xx}(k)\right)^{1/p}}}, \quad (18)$$

where p is a positive integer [the value of $(\omega_{xy})_{\text{opt}}$ is determined analogously].

Figure 3 shows the QMSA spectra of $(Cd_{1-x}Zn_x)_3As_2$ ($x = 0.45$) at 1.6, 19, 40, and 120 K. In the spectra, the concentration of each type of carrier j is

$$n_j \approx \sum_{i=1}^{i_j}(\sigma_i - \sigma_{i-1})/(e\mu_i),$$

i.e., the weighted sum of all carriers for the jth peak. The bulk concentrations of carriers and their mobilities are shown in Table I. It can be seen that there are two types of holes with different mobilities in the temperature range of 1.6–19 K; however, with increasing temperature, just one type of carrier is observed. It can be assumed

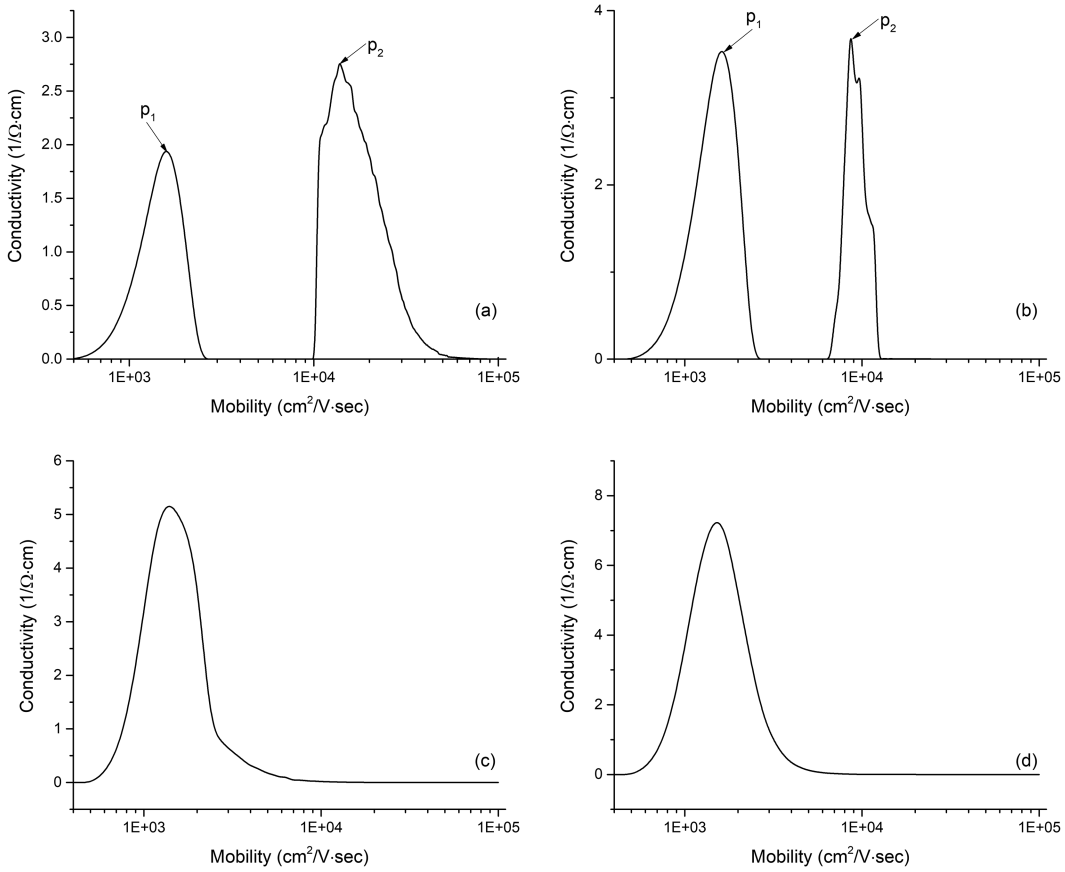

FIG. 3. QMSA spectra of $(Cd_{1-x}Zn_x)_3As_2$ ($x = 0.45$) at different temperatures: (a) 1.6 K, (b) 19 K, (c) 40 K, and (d) 120 K.

TABLE I. Concentrations and mobilities of carriers for $(Cd_{1-x}Zn_x)_3As_2$ (x = 0.45) at different temperatures.

	Concentration (cm^{-3})		Mobility ($cm^2\ V^{-1}\ s^{-1}$)	
Temperature (K)	Heavy	Light	Heavy	Light
1.6	1.8×10^{18}	7.7×10^{17}	1.6×10^3	1.6×10^4
19	1.7×10^{18}	5.2×10^{17}	1.6×10^3	8.6×10^3
40	5.2×10^{18}		1.2×10^3	
120	7.7×10^{18}		1.2×10^3	

that up to about 19 K, $(Cd_{1-x}Zn_x)_3As_2$ (x = 0.45) contains two types of holes, namely, light and heavy holes.

The concentration of heavy carriers is almost constant between 16 and 19 K and then increases rapidly with increasing temperature above 40 K, whereas their mobility decreases with increasing temperature above 40 K. On the other hand, the concentration of light carriers decreases with increasing temperature above 40 K, while their contribution to conductivity decreases and is no longer visible in the mobility spectrum. Our results are in qualitative agreement with those of the Bodnar model. That model is a generalization of the three-level Kane model for narrow-gap semiconductors with a tetragonal crystal structure within the *kp* approximation and is used to describe the band structure of many II_3–V_2 semiconductors, such as Cd_3As_2 and Zn_3As_2. According to the band structure model, the direct-gap *p*-type semiconductor Zn_3As_2 contains bands of both light and heavy holes,[14] which is consistent with our results.

IV. CONCLUSIONS

Using the modified Bridgman method, we have obtained single crystals of the $(Cd_{1-x}Zn_x)_3As_2$ (x = 0.45) solid solution. We have found by powder x-ray analysis that the single crystals belong to the α''' phase with space group $I4_1/amd$ and lattice parameters $a = b$ = 8.56(5) Å and c = 24.16(6) Å. We are the first to study the temperature dependence of the electrical conductivity and magnetoresistance of the α''' phase of the $(Cd_{1-x}Zn_x)_3As_2$ solid solution in the temperature range of 1.6–320 K and in the presence of a magnetic field from 0 to 10 T. The spectrum of charge carriers (Fig. 3) has been analyzed in the temperature range of 1.6–120 K by the QMSA method. It has been found that at temperatures of 1.6–19 K, two types of holes with different mobilities are present in the samples, while with increasing temperature, just one type of carrier is observed in the spectrum. It can be assumed that according to the Bodnar band model,[14] two types of holes are present in $(Cd_{1-x}Zn_x)_3As_2$ (x = 0.45), namely, light and heavy holes. The concentration of heavy carriers is almost constant (1.7×10^{18}–$1.8 \times 10^{18}\ cm^{-3}$) between 1.6 and 19 K and then increases rapidly with increasing temperature above 40 K. On the other hand, the contribution of light carriers to conductivity decreases and is no longer visible in the mobility spectrum. The mobility of heavy carriers decreases with increasing temperature above 40 K (Table I).

ACKNOWLEDGMENTS

This work was partially supported by the Ministry of Science and Higher Education of the Russian Federation (Grant No. 0851-2020-0035). It was financially supported by a Program of the Ministry of Education and Science of the Russian Federation for higher education establishments [Project No. FZWG-2020-0032(2019-1569)].

DATA AVAILABILITY

The data that support the findings of this study are available within the article.

REFERENCES

[1] E. K. Arushanov, "II_3V_2 compounds and alloys," Prog. Cryst. Growth Charact. Mater. **25**, 131–201 (1992).
[2] W. Zdanowicz and L. Żdanowicz, "Semiconducting compounds of the AIIBV group," Annu. Rev. Matter. Sci. **5**, 301–328 (1975).
[3] J. Misiewicz *et al.*, "Zn_3P_2—A new material for optoelectronic devices," Microelectron. J. **25**, xxiii–xxviii (1994).
[4] D. Stepanchikov and S. Shutov, "Cadmium phosphide as a new material for infrared converters," Semicond. Phys., Quantum Electron. Optoelectron. **9**, 40–44 (2006).
[5] T. Burgess *et al.*, "Zn_3As_2 nanowires and nanoplatelets: Highly efficient infrared emission and photodetection by an earth abundant material," Nano Lett. **15**, 378–385 (2015).
[6] Z. Wang, H. Weng, Q. Wu, X. Dai, and Z. Fang, "Three-dimensional Dirac semimetal and quantum transport in Cd_3As_2," Phys. Rev. B **88**, 125427 (2013).
[7] M. Neupane *et al.*, "Observation of a three-dimensional topological Dirac semimetal phase in high-mobility Cd_3As_2," Nat. Commun. **5**, 3786–3793 (2014).
[8] H. Lu, X. Zhang, Y. Bian, and S. Jia, "Topological phase transition in single crystals of $(Cd_{1-x}Zn_x)_3As_2$," Sci. Rep. **7**, 3148 (2017).
[9] V. S. Zakhvalinskii, T. B. Nikulicheva, E. A. Pilyuk, E. Lähderanta, M. A. Shakhov, O. N. Ivanov, E. P. Kochura, A. V. Kochura, and B. A. Aronzon, "Transport evidence of mass-less Dirac fermions in $(Cd_{1-x-y}Zn_xMn_y)_3As_2$ ($x + y$ = 0.4)," Mater. Res. Express **7**(4), 015918 (2020).
[10] O. Ivanov, V. Zakhvalinskii, T. Nikulicheva, M. Yaprintsev, and S. Ivanichikhin, "Asymmetry and parity violation in magnetoresistance of magnetic diluted Dirac–Weyl semimetal $(Cd_{0.6}Zn_{0.36}Mn_{0.04})_3As_2$," Phys. Status Solidi RRL **12**(6), 1800386 (2018).
[11] L. A. Saypulaeva, M. M. Gadzhialiev, A. G. Alibekov, N. V. Melnikova, V. S. Zakhvalinskii, A. I. Ril', S. F. Marenkin, T. N. Efendieva, I. V. Fedorchenko, and A. Yu. Mollaev, "Effect of hydrostatic pressures of up to 9 GPa on the galvanomagnetic properties of Cd_3As_2–MnAs (20 mol % MnAs) alloy in a transverse magnetic field," Inorg. Mater. **55**, 873–878 (2019).
[12] W. Zdanowicz, K. Lukaszewicz, and W. Trzebiatowski, "The crystal structure of the semiconductor system Cd_3As_2–Zn_3As_2," Bull. Acad. Polon. Sci. Ser. Sci. Chim. **12**, 169–176 (1964).
[13] G. F. Volodina, V. S. Zakhvalinskii, and V. Kh. Kravtsov, "Crystal structure of $\alpha'''(Zn_{1-x}Cd_x)_3As_2$ (x = 0.26)," Crystallogr. Rep. **58**, 563–567 (2013).
[14] E. K. Arushanov, A. F. Knyazev, A. N. Naterpov, and S. I. Radautsan, "Composition dependence of the band gap of $Cd_{3-x}Zn_xAs_2$," Sov. Phys. Semicond. **17**, 759–761 (1983).
[15] W. J. Turner, A. S. Fischler, and W. E. Reese, "Physical properties of several II–V semiconductors," Phys. Rev. **121**, 759–767 (1961).
[16] M. J. Aubin, "Transport properties of n type $Cd_{3-x}Zn_xAs_2$ alloys," Can. J. Phys. **53**, 1333–1337 (1975).
[17] J. Antoszewski, D. J. Seymour, L. Faraone, J. R. Meyer, and C. A. Hoffman, "Magneto-transport characterization using quantitative mobility-spectrum analysis," J. Electron. Mater. **24**, 1255–1262 (1995).

[18]J. R. Meyer, C. A. Hoffman, F. J. Bartoli, D. A. Arnold, S. Sivananthan, and J. P. Fauri, "Methods for magnetotransport characterization of IR detector materials," Semicond. Sci. Technol. **8**, 805–823 (1993).
[19]J. R. Meyer, C. A. Hoffman, J. Antoszewski, and L. Faraone, "Quantitative mobility spectrum analysis of multicarrier conduction in semiconductors," J. Appl. Phys. **81**, 709–713 (1997).
[20]I. Vurgaftman, J. R. Meyer, C. A. Hoffman, D. Redfern, J. Antoszewski, L. Faraone, and J. R. Lindemuth, "Improved quantitative mobility spectrum analysis for Hall characterization," J. Appl. Phys. **84**, 4966 (1998).
[21]E. K. Arushanov, "Crystal growth and characterization of II_3V_2 compounds," Prog. Cryst. Growth Charact. **3**, 211–255 (1981).
[22]W. Kraus and G. Nolze, "POWDER CELL – a program for the representation and manipulation of crystal structures and calculation of the resulting X-ray powder patterns," J. Appl. Crystallogr. **29**, 301–303 (1996).
[23]J. A. Dean, Lange's Handbook of Chemistry, 15th ed. (McGraw-Hill, New York, 1999), pp. 4.30–4.34.
[24]L. E. Soshnikov, V. M. Trukhan, and S. F. Marenkin, "Temperature-Dependent elastic constants and dielectric properties of $(Zn_{1-x}Cd_x)_3(P_{1-y}As_y)_2$ crystals," Inorg. Mater. **39**, 317–322 (2003).
[25]J. R. Meyer, C. A. Hoffman, F. J. Bartoli, J. M. Perez, J. E. Furneaux, R. J. Wagner, R. J. Koestner, and M. W. Goodwin, "Magnetotransport and farinfrared magnetooptical studies of molecularbeam epitaxially grown HgTe," J. Vac. Sci. Technol., A **6**, 2775 (1988).
[26]B. A. Aronzon and I. M. Tsidilkovskii, "Magnetic-field-induced localization of electrons in fluctuation potential wells of impurities," Phys. Status Solidi B **157**, 17 (1990).
[27]W. A. Beck and J. R. Anderson, "Determination of electrical transport properties using a novel magnetic field dependent Hall technique," J. Appl. Phys. **62**, 541 (1987).
[28]Z. Dziuba and M. Górska, "Analysis of the electrical conduction using an iterative method," J. Phys. III **2**, 99 (1992).
[29]J. Kiusalaas, *Numerical Methods in Engineering with Python 3* (Cambridge University Press, Cambridge, 2013).